Applied Mathematics & Information Sciences
An International Journal

http://dx.doi.org/10.18576/amis/130508

Investigation of Pinched Hysteresis of a Memristor Emulator Under Ferroresonance

S. Poornima * *and C. Pugazhendhi Sugumaran*

Division of High Voltage Engineering, Anna University, Chennai, India

Received: 23 Mar. 2019, Revised: 12 Apr. 2019, Accepted: 26 Apr. 2019
Published online: 1 Sep. 2019

Abstract: The frequent occurrence of ferroresonance phenomenon has destructive effects in distribution systems. The jump resonance accompanied by harmonics can be effectively mitigated using a nonlinear component. The upcoming memristor technology is applied in this work to control the ferroresonance in an inductive voltage transformer, which is used in a distribution substation. Due to non-commercialization of memristors, an emulator in the form of an electrolytic cell is developed. The set-up uses saturated copper sulfate ($CuSO_4$) solution as the electrolyte and copper electrodes having different cross sectional areas. Nonlinearity is realized in the form of the pinched hysteresis loop in the developed memristor emulator. The required memristance is obtained by using a proper design of the $CuSO_4$ set-up. The nonlinear resonance is indicated by the sudden jump up of 30 V and jump down of 15 V in the secondary winding of the transformer. The current-voltage relation of the emulator is compared with that of an ideal memristor under normal and ferroresonance conditions. The behavior of $CuSO_4$ memristor is validated against the HP memristor experimentally in terms of nonlinearity index and phase shift values.

Keywords: Memristor, Pinched hysteresis, Ferroresonance, Inductive voltage transformer, Mitigation

1 Introduction

The memristor was identified as the fourth basic circuit element by Chua in 1971. The peculiar properties of memristors proved the existence of this fundamental element, next to resistors, inductors and capacitors [1]. Like the passive elements, the memristor holds an axiomatic relation between charge and flux in an electric circuit. A group of scientists at HP Laboratories discovered that a sandwiched titanium oxide and platinum device possessed the properties shown by Chua's observations [2]. A memristor exhibits the unique memory property of possessing a present value based on its past. This non-volatile property depends on the state of the resistance offered against the ionic movement in the device [3]. Strange voltage-current characteristics is the main fingerprint of an ideal memristor. This characteristic is a hysteresis curve with a pinched nature at its origin. This pinching nature under a periodic excitation depends on the supply frequency and a control variable, either voltage or current of the device. The hysteresis curve is nonlinear under very low frequencies and linear at high frequencies.

The invention of HP's memristor as a physical device invoked a new research trend in identifying memristor behavior in biological constituents, like human skin and plants [4–6], electronic components, such as programmable circuits, JFETs and operational amplifiers [7–10], and chemical components, like discharge lamps, coherers, etc. [11, 12]. A special attention is given to memristor properties in the field of nanomaterials [13]. The high cost of fabrication and realization difficulties are the driving forces for the development of many emulator devices in the above mentioned areas. Although many memristor emulators possess pinched hysteresis characteristics, they fail to have the memory property. Regardless of their limitations, memristor emulators find potential applications in memory devices, ADC/DAC circuits, oscillators, voltage dividers and switches [14–20]. With the implementation of memristor emulators, the mutation of memristors to meminductors and memcapacitors has also emerged [21–23]. In the near future, memelements will be available in various ratings, like existing passive elements. The memristor or its mutuator as a nonlinear

* Corresponding author e-mail: poojeyaani@gmail.com

element with memory property is likely to enhance many circuit's topologies and performance.

In this study, a memristor emulator using a saturated aqueous solution of Copper sulphate ($CuSO_4$) is proposed to suppress the ferroresonance overvoltage in an inductive voltage transformer. The pinched hysteresis behavior of the memristor emulator against various parameters is validated with respect to the fundamental memristor model. The results obtained in this investigation proved that the memristor could be employed as a nonlinear resistor in high voltage applications.

2 Memristor

The property that relates charge (q) and flux (φ) is unique in an ideal memristor. It may have the control variable as charge (flux) if it is current (voltage) controlled. Charge-controlled memristor models describe this relation as a function of charge in terms of current, i flowing in the circuit [24]:

$$\varphi = \hat{\varphi}(q) \tag{1}$$

Differentiating (1),

$$v = \frac{d\varphi}{dt} = \frac{d\hat{\varphi}(q)}{dq} \cdot \frac{dq}{dt} \tag{2}$$

where $R(q) = \frac{d\hat{\varphi}(q)}{dq}$ is a continuous differentiable function known as memristance. Then, Ohm's law becomes

$$V = R(q)i \tag{3}$$

In contrast, flux-controlled memristor models describe the charge flux relation as a function of flux in terms of voltage applied to the circuit:

$$q = \hat{q}(\varphi) \tag{4}$$

Differentiating (4),

$$i = \frac{dq}{dt} = \frac{d\hat{q}(\varphi)}{d\varphi} \cdot \frac{d\varphi}{dt} \tag{5}$$

where $G(\varphi) = \frac{d\hat{q}(\varphi)}{d\varphi}$ is a piecewise differentiable function known as memductance. According to Ohm's law,

$$i = G(\varphi)V \tag{6}$$

An expression for any passive element can be obtained from a general Eq. [25], as given by

$$y = a_1 x + (a_2 + a_3 x)\frac{dx}{dt} + (a_4 + a_5 x)\int_0^t x(\tau)d\tau \tag{7}$$

where a_1 to a_5 are scaling coefficients and x and y are the input and output signals, respectively. Eq. (7) describes the normal, differentiated and integrated behavior of the input signal. Under a sinusoidal supply, the input can be given as

$$x(t) = psin(\omega t + \theta) \tag{8}$$

$$\frac{dx}{dt} = p\omega\cos(\omega t + \theta) = \pm\omega\sqrt{p^2 - x^2} \tag{9}$$

$$\int_0^t x(\tau)\,d\tau = \frac{1}{\omega}pcos\theta \mp \sqrt{p^2 - x^2} \tag{10}$$

Substituting (8)–(10) in (7),

$$y = a_1 x + p(a_4 + a_3 x)\frac{\cos\theta}{\omega} \pm \left\{\left(a_5\omega - \frac{a_3}{\omega}\right)x + \left(a_2\omega - \frac{a_4}{\omega}\right)\right\}\sqrt{p^2 - x^2} \tag{11}$$

Due to odd symmetry, Eq. (11) becomes

$$y = a_1 x + p(a_4 + a_3 x)\frac{\cos\theta}{\omega} \tag{12}$$

Resistance can be obtained using Eq. (11) when the scaling constants other than a_1 become zero to give a linear relation.

$$y = a_1 x \tag{13}$$

Inductance can be realized by zeroing the scaling constants a_1, a_3, a_4 and a_5 in Eq. (11) to its voltage current relation as

$$y = p\omega\cos(\omega t + \theta)\cdot a_2 \tag{14}$$

Similarly, capacitance can be obtained by making $a_4 \neq 0$ in Eq. (11) and the voltage current relation will be

$$y = pa_4\frac{\cos\theta}{\omega} \tag{15}$$

As per Eq. (7), a general equation for the memristance property based on the pinched hysteresis property can be written as

$$y(t) = x(t)\left[a_1 + a_3\int_0^t x(\tau)\,d\tau\right] + a_2\frac{dx(t)}{dt} \tag{16}$$

where a_1 represents the initial state of the memristor and defining a_2 as zero in Eq. (16) gives the symmetry nature.

For a voltage-controlled memristor, the output $y(t) = \frac{i(t)}{V_b G_b}$ for the period (T) with input $(t) = \frac{v(t)}{V_b}$, arbitrary values of transconductance (G_b) and the reference voltage (V_b), the current voltage equation is given by

$$i(t) = \pm v(t)G_b \pm G_b\frac{v(t)}{TV_b}\varphi(t) \tag{17}$$

The memductance $\frac{i(t)}{v(t)} = G_m$ is also given by

$$G_m = \pm G_b \pm G_b\left(\frac{1}{TV_b}\right)\varphi(t) \tag{18}$$

With the flux $\varphi(t)$, Eq. (18) gives two incremental and two decremental values of memductance.

For a current-controlled memristor, the input $x(t) = \frac{i(t)}{I_b}$ produces the output $y(t) = \frac{v(t)}{I_b R_b}$ with the arbitrary values of memristance (R_b) and the reference current (I_b), the voltage current equation will be given by

$$v(t) = \pm i(t)R_b \pm R_b \left(\frac{i(t)}{TI_b}\right) q(t) \tag{19}$$

The memristance $\frac{v(t)}{i(t)} = R_m$ is also written as

$$R_m = \pm R_b \pm R_b \left(\frac{1}{TI_b}\right) q(t) \tag{20}$$

Eq. (20) gives two incremental and decremental values of memristance at the given charge $(q(t))$. For any component-based memristor emulator, Eqs. (18) and (20) can give memristance and memductance values, respectively.

For an ideal voltage-controlled memristor, the memductance versus flux state map implies Ohm's law as

$$i = G(x)V \tag{21}$$

where x is the flux considered as a state variable that shows the memductance value dynamically. As the memductance gives the slope of the flux–charge relation, the minimum and maximum values can be obtained from the state map.

For unsymmetrical behavior, the differentiation term has to be taken into consideration for the calculation of the G_m and R_m values. The pinch point should be the origin for the symmetrical hysteresis at any frequency. In practice, the pinch point may be translated due to the parasitic effects of the DC component of supply, inductance, capacitance and current source of the emulator circuit [26].

3 Electrochemical Memristor Emulator

Memristive behavior is observed in cyclic voltammetry of some liquids. The pinched hysteresis nature depends upon the electrical capacity of the chosen electrode and electrolyte properties.

3.1 Theory

The memristive property is found in electrolytic cell arrangements with dissimilar copper electrodes and a saturated $CuSO_4$ aqueous solution [27]. Two enamel coated copper electrodes of different thicknesses are chosen. The tip of the electrodes is cleaned properly so that the electric field is focused when connected to a voltage source. The thinner electrode is chosen as the anode as the current density near the anode electrolyte should be more. The thicker electrode is chosen as the cathode so that the chemical reactions at the cathode electrolyte interface should be asymmetrical. The distance between the electrodes can be as close as possible to ensure easy transport of ions. The ratio of the conducting area of the electrodes must be good enough to obtain pinched hysteresis.

Copper Sulfate Pentahydrate ($CuSO_4.5H_2O$) is added to the distilled water after proper measurement. It is allowed to dissolve in distilled water at room temperature until the salt precipitates at the bottom of the beaker. The solution is stirred for 10 min using a magnetic stirrer. A drop of concentrated sulfuric acid (H_2SO_4) is added to make the solution clear and transparent. The concentration of $CuSO_4$ can be verified using its standard solubility curve.

An alternating voltage is applied to the setup so that the current density at the anode is enough to produce a strong field. The electric field in turn produces self-ionization of water molecules. The water molecule is dissociated into H^+ and OH^- ions. The OH^- ions react with a copper atom of the anode and deposits its oxide on the electrode surface.

$$Cu + H_2O \rightarrow CuO + 2H^+ + 2e^- \tag{22}$$

The behavior of the electrolyte will not be the same for different types of excitation. Meanwhile, the electrolyte under periodic excitation dissociates as Cu^{2+} and SO_4^{2-} ions. The Cu^{2+} ions get attracted towards the negative terminal of the source, take two electrons and become neutralized. The SO_4^{2-} reacts with the copper atoms of the anode and forms $CuSO_4$, which is dissolved in water over again.

$$CuSO_4 \rightarrow Cu^{2+} + SO_4^{2-} \tag{23}$$

At the anode,

$$Cu^{2+} + 2e^- \rightarrow Cu \tag{24}$$

At the cathode,

$$SO_4^{2-} + Cu \rightarrow CuSO_4 + 2e^- \tag{25}$$

These reactions are repeated and maintain the net charge in the setup as zero. These reactions cannot occur at the cathode as a very small electric field exists at its electrolyte interface. The hydrogen ions of (22) react with SO_4^{2-} ions to form sulfuric acid.

$$2H^+ + SO_4^- \leftrightarrow H_2SO_4 \tag{26}$$

The thickness of CuO deposited on the anode surface has a semiconductor property and resists the electron flow. The resistivity of CuO deposition depends on the past value of electric current between the electrodes. Hence, the setup is said to have the memory property. However, the negative supply of voltage can reduce the CuO deposition and hence loses memory property. However, the prolonged operation of this setup under constant

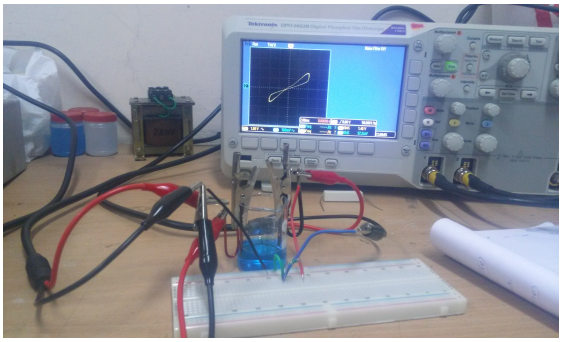

Fig. 1: $CuSO_4$ setup with pinched hysteresis

voltage maintains the memristive action. The sulfuric acid (H_2SO_4) of (26) dissolves the CuO film formed on the anode surface and traps hydrogen gas at the cathode. The hydrogen gas may create unwanted pressure within the setup.

3.2 Realization of Pinched Hysteresis Characteristics

The main fingerprint of the memristor is the pinched nature hysteresis at the zero crossing point. The pinched hysteresis area is directly proportional to the amplitude of the source. The hysteresis lobe area of the first and third quadrant may be asymmetrical due to the presence of reactive elements in series or parallel with the memristor emulator. This also depends upon the properties of the components used to mimic the memristor behavior.

The pinched hysteresis is also said to be peculiar due to its dependency on the supply frequency. The Lissajous curve obtained is shown in Fig. 1. At very low frequencies, the hysteresis curve is nonlinear. As the frequency is increased gradually, the hysteresis curve may lose its pinch nature but remains nonlinear. At high frequencies, the characteristic is absolutely linear. Since the hysteresis nature is indirectly proportional to high values of frequency, the lobe area shrinks and finally appears as a slope line. The developed memristor emulator is supplied in the frequency ranges from 1 mHz to 15 MHz.

4 Mitigation of Fundamental Ferroresonance

Ferroresonance is a nonlinear resonance phenomenon that occurs between a low loss or unloaded transformer and system capacitance in a power system. It is an unpredictable event recorded in HVDC stations, distribution systems, microgrids [28–30] and it needs to be mitigated.

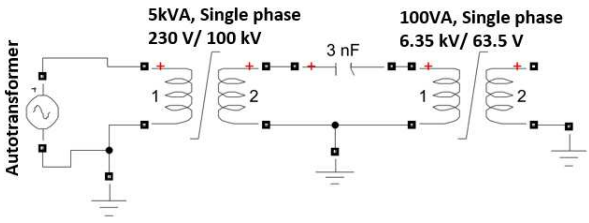

Fig. 2: Experimental setup for ferroresonance inception

4.1 Inception of Ferroresonance

There are four modes of ferroresonance: fundamental, quasi, subharmonic and chaotic. Among the four modes, the most frequent kind is the fundamental mode characterized by distorted overvoltages and overcurrent at the fundamental frequency. The occurrence can be realized as a sudden jump-up and jump-down phenomenon. Hence, it is also known as jump resonance.

The fundamental ferroresonance was intentionally created in a 100 VA, 6.35 kV/63.5 V rated single phase inductive voltage transformer. The capacitance of 3 nF to induce ferroresonance was identified using Rudenberg's graphical method [31].

The inductive voltage transformer was gradually energized by an autotransformer through a high voltage transformer and the chosen capacitor, as shown in Fig. 2 Ferroresonance was realized when the secondary voltage of the transformer was raised from 55V to 84.86 V. The secondary voltage recorded using DPO 2022B shows distortion in the waveform. Along with the fundamental component, the voltage had considerable third and fifth order harmonic components. This sudden jump up was also reflected in the primary voltage and current. While gradually reducing the voltage to zero, the secondary voltage suddenly drops from 76.5 to 61.3 V.

4.2 Suppression Using Memristor Emulator

The fundamental ferroresonance can be suppressed by the addition of 10% load to the transformer [32]. The factors that decide the required impedance are electrode configuration, electrolyte concentration and the distance between the electrodes. The ON/OFF ratio of the developed setup depends upon the CuO molecules deposited on the anode copper. The thickness of the copper cathode is chosen as five times that of the anode. The pinch nature does not occur below this ratio. The high current density at the anode with a strong electric field creates rapid deposition of CuO that provides the required resistance. The copper anode is connected to the phase terminal of the secondary of the inductive voltage transformer. The copper cathode and the neutral of the transformer is connected to earth.

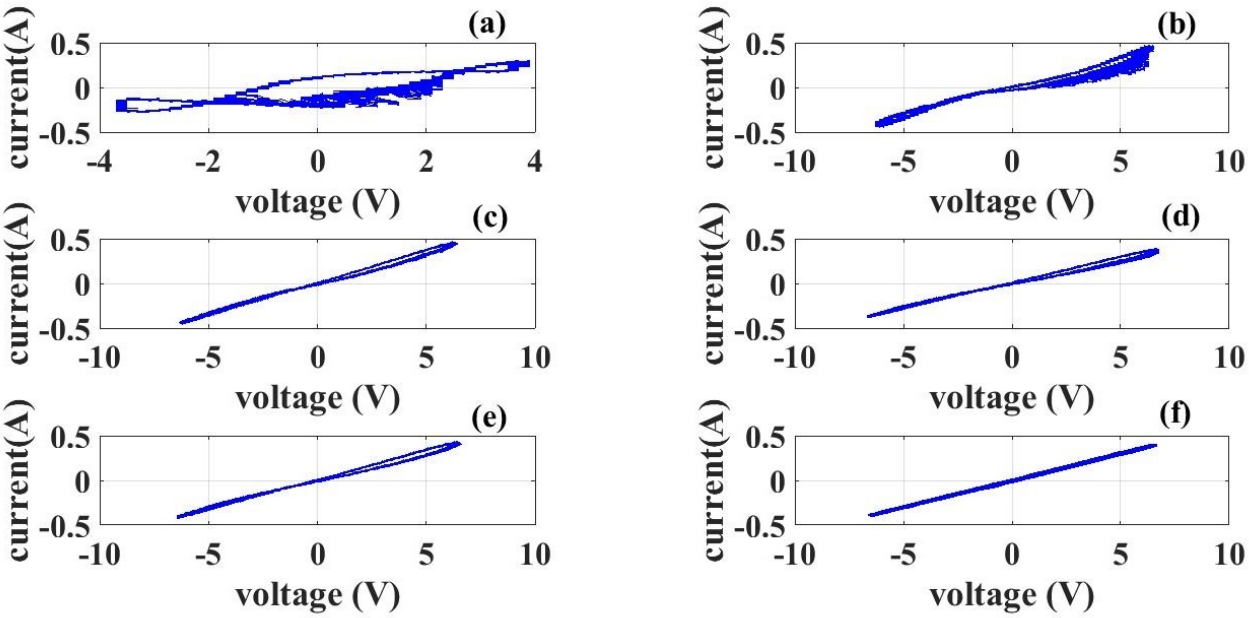

Fig. 3: Pinched hysteresis of $CuSO_4$ memristor emulator at frequencies of (a) $<$ 10 Hz, (b) 73 Hz, (c) 250 Hz, (d) 1 kHz, (e) 2 kHz and (f) 11 kHz

During the fundamental ferroresonance, the $CuSO_4$ setup is connected across the secondary of the transformer. The raised voltage has been reduced to 56 V as the memristor emulator took 171 mA. The secondary voltage of the transformer retains its normal magnitude and shape with the developed memristor emulator. The absence of harmonic components in the secondary voltage waveform proved the suppression of ferroresonance.

5 Results and Discussion

In future, the memristor may be available in different ratings, like a resistor. The nonlinear property of the memristor may prompt its application in transformer protection. The main contribution of this study is the application of a memristor emulator as a nonlinear load. Besides the memory property, the pinched hysteresis of the developed memristor emulator has been verified experimentally. In addition, the pinched nature of the memristor emulator has been verified analytically with Eqs. (16)–(18), as discussed earlier.

The nonlinearity index and phase shift with respect to voltage and current curves are also considered as parameters of nonlinear measurements [33]. The nonlinearity can be calculated with the following:

$$\text{nonlinearity} = \frac{(I_M - I_{0.5V_M})}{(I_{0.75V_M} - I_{0.5V_M})} \tag{27}$$

An index of nonlinearity of less than 2 indicates linear characteristics and vice versa.

The deviations from the ideal characteristics may be due to the parasitic effect of the DC component along with the voltage applied to the memristor emulator circuit. The pinching may not occur exactly at zero crossing. The area of pinched hysteresis may be asymmetrical. The behavior of the memristor emulator has been analyzed under various factors in the following discussion.

5.1 Different Frequencies

The Lissajous curve of the developed emulator at different frequencies has been obtained using an Agilent function generator. The current measurement has been taken across a 10 Ω resistance. The pinched nature starts at 30 Hz and vanishes at 10 kHz. The Lissajous curve has two pinch points at 10 Hz whereas the pinch point from 30 Hz is slightly shifted from the origin point, as shown in Fig. 3. The hysteresis has a pinching effect in the third quadrant. This is due to the parasitic effect of the DC component present in the supply voltage.

Fig. 4 compares the nonlinearity indexes calculated as per Eq. (27) for the frequencies varied until the Lissajous pattern lost its pinching nature. The expected ideal nonlinearity could not be produced experimentally, except at 11 kHz. Fig. 5 shows a comparison of the phase shift of the memristor emulator at various frequencies. The calculated phase shift values mismatched the experimental values. The nonlinearity and phase shift

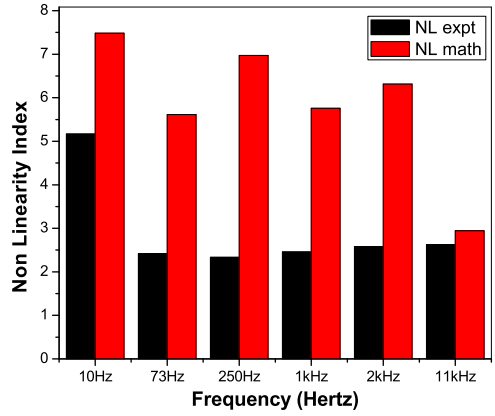

Fig. 4: Nonlinearity index comparison at different frequencies

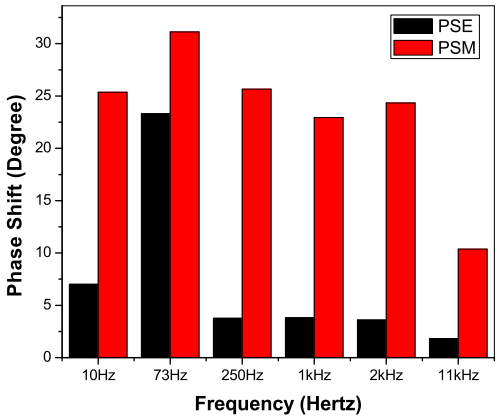

Fig. 5: Phase shift comparison at different frequencies

decreases as the frequency increases, which should be true to satisfy the frequency dependent nature of a memristor.

5.2 Different Supply Voltage Magnitudes

The CuSO4 setup has been supplied with a 50 VA, 230 V/110 V rated single phase transformer in order to check its performance in the range of 50–80 Vrms. As the ferroresonance dealt with the 63.5 V transformer, the test voltage fell within this range. The hysteresis lobe areas are small and asymmetrical, as shown in Fig. 6 The signals stored in DPO2022B are processed at the sampling frequency of 1.25 MHz and are compared with Fouda's I–V relation (18) using Matlab. The voltage is supplied at 50Hz as the fundamental ferroresonance is concerned at power frequency only.

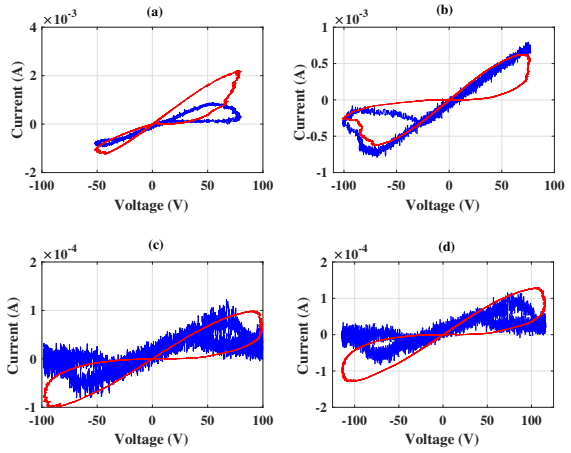

Fig. 6: Pinched hysteresis at supply voltages of (a) 50 V (b) 60 V (c) 70 V and (d) 80 V. The blue curve indicates the lissajous curve of memristor emulator obtained with experiment results. The red curve indicates the lissajous curve of ideal memristor obtained analytically

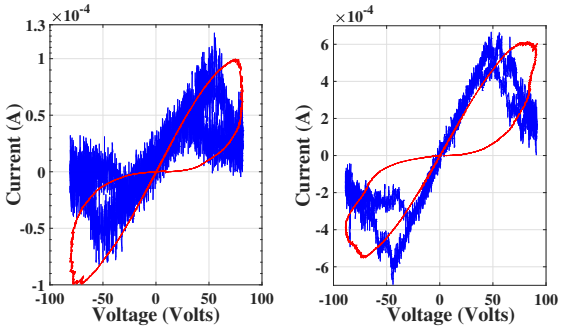

Fig. 7: Pinched hysteresis at supply voltage of 56 V under (a) normal (b) during ferroresonance mitigation. The blue curve indicates the lissajous curve of memristor emulator obtained experimentally. The red curve indicates the lissajous curve of ideal memristor obtained analytically

Table 1: RMSE at different supply voltages

Voltage (V_{rms})	RMSE
50 V	6.2366e-04
60 V	3.5899e-04
70 V	4.7330e-05
80 V	6.2775e-05

The difference between the two signals of each voltage is measured in terms of root mean square error (RMSE). The deviation from the ideal I-V relation is listed in Table 1. The conductance value of the developed memristor emulator decreases from 3.44e-05 to 1.64e-06 as the applied voltage increases from 50 to 80 V.

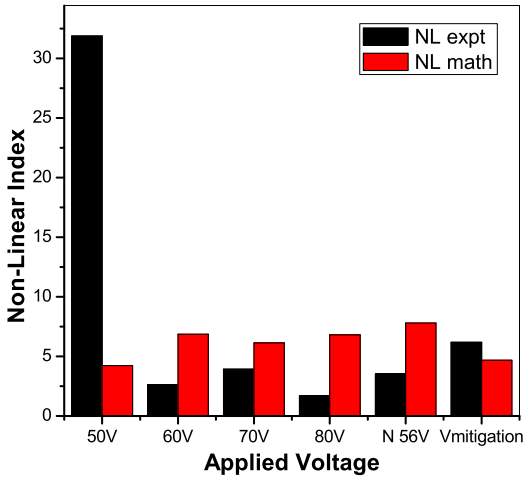

Fig. 8: Nonlinearity index under different voltages

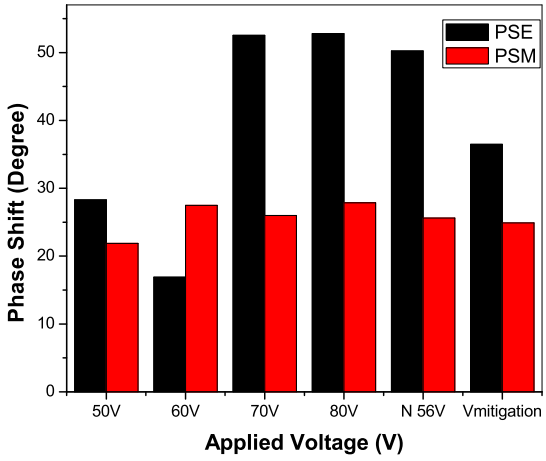

Fig. 9: Phase shift under different voltages

5.3 Suppression of Ferroresonance

During ferroresonance, the memristor emulator was connected as a nonlinear resistor in order to damp the oscillations. The performance of the developed emulator against the mathematical expression is shown in Fig. 7. The input voltage to the memristor emulator is a distorted sinusoidal measured at a sampling frequency of 125 kHz. In order to find the exact pinching point and ease comparison with the ideal equation, the signal has been smoothed using Gaussian method. The areas of the hysteresis curve in the first and third quadrants are not symmetrical. This may be due to the parasitic inductance present in the practical circuit.

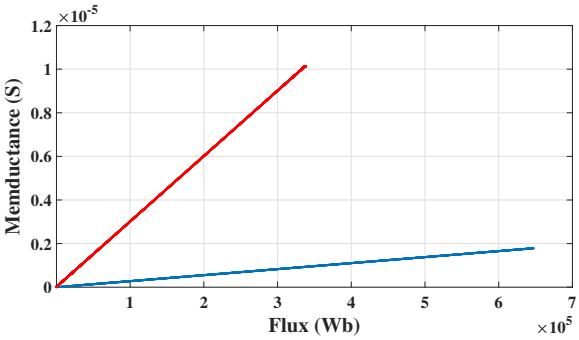

Fig. 10: Memductance variation during normal and ferroresonance mitigation conditions. The blue line represents the transconductance with a pure sinusoidal excitation. The red line represents the transconductance under a distorted, harmonic contained nonsinusoidal excitation

The RMSE value of pinched hysteresis during mitigation of ferroresonance has been found to be 2.670e-04, whereas under normal conditions, the error has been found to be 3.128e-05. The comparison of nonlinearity index and phase shift values for the chosen voltages among the simulation and experimental results are shown in Figs. 8 and 9 respectively. The nonlinearity index values calculated as per Eq. (27) for the chosen voltages are compared among the simulation and experimental results. The index has been found to be high during 50 V and mitigation against ferroresonance. The results implicates that the nonlinearity decreases experimentally due to practical factors.

The phase shift between the voltage and current of the memristor emulator can be considered as important in order to understand the pinching nature. The obtained results infer that more phase shift occurs practically than the analytical cases, except at 60 V.

The fundamental state map for a voltage-controlled memristor is obtained between the memductance and flux of the circuit. The maximum memductance during mitigation is found to be 1.0123e-05 S when compared to 1.7846e-06 S of normal condition. During ferroresonance, the abrupt increase in the memductance or transconductance at its nonlinear input voltage is shown in Fig. 10. The frequency dependence of memductance may cause this increase due to nonsinusoidal voltage obtained during ferroresonance.

6 Conclusion

An attempt has been made to apply the future memristor technology in the mitigation of fundamental ferroresonance. In order to check the response of memristor emulator, a single-phase inductive voltage transformer has been chosen. Rudenberg's graphical

method is applied to identify the value of capacitance required to create ferroresonance intentionally.

Among the proposed memristor emulator circuits in the literature, the $CuSO_4$-based setup is suitable for working under an 80 V supply. The pinched hysteresis behavior is verified under various voltage magnitudes and frequencies for the $CuSO_4$ setup. The requirement of suppression is appropriately considered in the design of an emulator circuit.

The nonlinear behavior of the proposed device is verified in terms of its pinched hysteresis characteristics, such as nonlinearity index, phase shift and root mean square error. The memductance of the developed and ideal memristor is compared under normal and transient conditions. The memory property of the developed emulator could have been analyzed using SEM analysis in terms of copper oxide deposition on the anode of the $CuSO_4$ setup, which may be a different aspect of research.

On successful mitigation of ferroresonance in an inductive voltage transformer using the proposed circuit, the secondary voltage is recovered by 96.3%. A current voltage relation of ideal memristor is used to verify the quantification of pinched hysteresis nature of the developed emulator circuit.

References

[1] L.O. Chua, Memristors: The missing circuit element, *IEEE Transactions on Circuit Theory*, **18**(5), 507–519 (1971).

[2] R. Williams, How we found memristor, *IEEE spectr.*, **45**, 28–35 (2008).

[3] M.D. Pickett et al., Switching dynamics in titanium dioxide memristive devices, *Journal of Applied Physics*, **106**, 074508 (2009).

[4] O.G. Martinsen, S. Grimnes, C.A. Lütken and G.K. Johnsen, Memristance in Human skin, *Journal of Physics: International Conference on Electrical Bioimpedance Series*, **224**, IOP Publishing Ltd. (2010).

[5] A.G. Volkov, C. Tucket, J. Reedus, M.I. Volkova, V.S. Markin and L. Chua, Memristors in plants, *Plant Signaling & Behavior*, **9**, 28152(1–7) (2014).

[6] A.G. Volkov et al., Memristors in the electrical network of Aloe vera L, *Plant Signaling & Behavior*, **9**, e29056 (2014).

[7] Y.V. Pershin and M. Di Ventra, Practical approach to programmable analog circuits with memristors, *IEEE Transactions on Circuits and Systems—I: Regular Papers*, **57**(8), 1857–1864 (2010).

[8] D. Biolek, V. Biolek, Z. Kolka and Z. Biolek, Passive fully floating emulator of memristive device for laboratory experiments, *Advances in Electrical and Computer Engineering*, 112–116 (2015).

[9] Olufemi A. Olumodefi and Massimo Gottardi, Emulating the physical properties of HP memristor using an aruduino and digital potentiometer, *12th IEEE Conference on PhD. Research in Microelectronics and Electronics* (2016).

[10] R. Stanely, *Memristors and Memristive Devices*, Springer Verlag Publishers, New York, 2014.

[11] D. Lin, S.Y. RonHui and L.O. Chua, Gas discharge lamps are volatile memristors, *IEEE Transactions On Circuits and Systems—I: Regular Papers*, **61**(7), 2066–2073 (2014).

[12] G. Gandhi, V. Aggrawal and L. Chua, Coherer is the elusive memristor, IEEE International symposium on Circuits and Systems (ISCAS) (2014).

[13] Byung Joon Choi et al., High speed and low energy nitride memristors, *Adv. Funct. Mater.*, **26**, 5290–5296 (2016).

[14] Y.V. Pershin, E. Sazonov and M. Di Ventra, Analogue to digital and digital to analogue conversion with memristive devices, *Electron. Lett.*, **48**(2), 73–74 (2012).

[15] M. Frasca, A. Farina and H. Griffiths, Effect of input noise on phase coherence in a lattice of memristors acting as a voltage divider, *Journal of Engineering*, **3**, 51–56 (2017).

[16] Y.V. Pershin and M. Di. Ventra, Teaching memory based elements via experiment based learning, *IEEE Circuits and Systems Magazine*, **12**(1), 66–74 (2012).

[17] Changhyuck Sung, Hyunsang Hwang and In Kyeong Yoo, Perspective: A review on memristive hardware for neuromorphic computation, *J. Appl. Phys.*, **124**, 151903 (2018).

[18] T.A. Wey and W.D. Jemison, Variable gain amplifier circuit using titanium dioxide memristors, *IET Circuits, Devices Syst.*, **5**(1), 59–65 (2011).

[19] H. Li and M. Hu, Compact model of memristors and its applications in computing systems, *Proceedings of the IEEE Design, Automation and Test in Europe Conference*, Dresden, Germany, March 8–12 (2010).

[20] M. Potrebic, D. Tosic and D. Biolek, Reconfigurable microwave filters using memristors, *International Journal of Circuit Theory and Applications*, **46**(21), 113–121, (2017).

[21] Y.V. Pershin and M. Di Ventra, Memristive circuits simulate memcapacitors and meminductors, *Electron. Lett.*, **46**, 517–518, (2010).

[22] D. Biolek and V. Biolkova, Mutator for transforming memristor into memcapacitor, *Electron. Lett.*, **46**, 1428–1429 (2010).

[23] Y.V. Pershin, Julian Martinez Rincon and M. Di. Ventra, Memory Circuit Elements: From Systems to Applications, *Journal of Computational and Theoretical Nanoscience*, **8**, 441–448 (2010).

[24] LO. Chua, The fourth element, *Proc. IEEE*, **100**, 1920–1927 (2012).

[25] Mohammed E. Fouda, Ahmed G. Radwan and Ahmed Elwakil, Memristor and Inverse Memristor: Modeling, Implementation and Experiments, in *Advances in Memristors, Memristive Devices and Systems*, (Eds.) Sundarapandian Vaidyanathan and Christos Volos (2017).

[26] Maheswar Pd Sah et al., A Generic Model of Memristors with Parasitic Components, *IEEE Transactions on Circuits and Systems–I: Regular Papers* **63**(3), 891–898 (2015).

[27] Farshad Merrikh Bayat and Meysam Parvizi, Practical method to make a discrete memristor based on the aqueous solution of copper sulfate, *Applied Physics A–Material Science and Processing*, Springer Publications, **122**(6), (2016).

[28] V. Valverde, G. Buigues, A.J. Mazón, I. Zamora and I. Albizu, Ferroresonant Configurations in Power Systems, *International Conference on Renewable Energies and Power Quality*, Spain (2012).

[29] D. Jacobson, L. Marti and R. Menzies, Modelling Ferroresonance in a 230 kV Transformer terminated Double Circuit Transmission line, *Proceedings of the International Conference on Power Systems Transients*, 451–456 (1999).
[30] M. Monadi, A. Luna, J.I. Candela, J. Rocabert, M. Fayezizadeh and P. Rodriguez, Analysis of Ferroresonance Effects in Distribution Networks with Distributed Source Units, *39th IEEE Conference on Industrial Electronic Society* (2013).
[31] R. Rudenberg, *Transient Performance of Electric Power Systems–Phenomenon in Lumped Networks*, McGraw-Hill, New York (1950).
[32] Ph. Ferracci. Ferroresonance. Application Note, [online] Cahier Technique Merlin Gerin no. 190 (1998). http://www.schneider-electric.com/cahier_technique/en/pdf/ect190.pdf
[33] O. Pabst, O.G. Martisen and L. Chua, The nonlinear properties of human skin make it as generic memristor, *Scientific Reports*, **15806**, 8 (2018). DOI: 10.1038/s41598-018-34059-6.

S. Poornima received her Bachelor in Electrical & Electronics Engineering from C. Abdul Hakeem College of Engineering, Vellore in 2003 and Master Degree in Power Systems engineering from Government College of Technology, Coimbatore in 2005. She has 10 years of teaching experience in engineering colleges. Currently she is a full time research scholar in Anna University, Chennai. Her area of interest includes Electrical Machines, study of ferroresonance in power systems.

C. Pugazhendhi Sugumaran (M'10-SM'16) is working as Associate Professor in the High voltage division of Anna University, Chennai. He obtained the B.E. degree in Electrical and Electronics Engineering from Government college of Engineering, Tirunelveli, affiliated to Manonmanium Sundaranar University, India in 1997 and M.E. degree in High-Voltage Engineering from Anna University, India in 2001. He was awarded Ph.D. in Electrical and Electronics Engineering from Anna University, India in 2011. His current areas of interest are Electromagnetic Interference, Nano Technology Application to High Voltage and Development of Nano Dielectric materials. He is the life member of Society of EMC and QCFI.